Lightning Propagation Through the Earth and its Potential for Methane Ignitions in Abandoned Areas of Underground Coal Mines

Thomas Novak, *Senior Member, IEEE*
The University of Alabama
Department of Civil and Environmental Engineering
Box 870205
Tuscaloosa, AL 35487

Thomas J. Fisher
National Institute of Occupational Safety and Health
Pittsburgh Research Laboratory
Cochrans Mill Road
P.O. Box 18070
Pittsburgh, PA 15236

Abstract. **Strong circumstantial evidence suggests that lightning has initiated methane explosions in abandoned and sealed areas of underground coal mines. The Mine Safety and Health Administration (MSHA) investigated several of these occurrences within recent years. The investigated explosions occurred at significant depths, ranging from 500 ft to 1200 ft. Data from the National Lightning Detection Network indicate a definite correlation between the times and locations of the explosions with those of specific lightning strikes. This paper addresses the question, "Can lightning cause potential differences capable of igniting methane-and-air mixtures at overburden depths at which underground coal mining occurs?" A mine depth of 600 ft was selected for this initial study. Computer simulations were performed, with and without the presence of a metal-cased borehole extending from the surface to the mine level. CDEGS™ software from Safe Engineering Services & Technologies, Ltd (SES) was used for the simulations.**

I. INTRODUCTION

Electrical shock, visible sparking from underground equipment, premature detonation of explosives, and methane explosions have been experienced in underground mines during thunderstorms. These incidents have been particularly well documented in shallow coal mines in South Africa [1, 2, 3], with the vast majority occurring at mining depths of 300 ft or less. In recent years, several methane explosions in the United States have also been attributed to lightning. However, these explosions occurred at depths ranging from 500 to 1200 ft, which are significantly deeper than any of the incidents experienced in South Africa.

The explosions in the United States took place in abandoned and sealed areas of underground coal mines. In some instances, steel-cased boreholes were located in the vicinity of the explosions. Data obtained from The National Detection Network were used to determine the number and magnitude of cloud-to-earth lightning strikes within a 10-mile radius of the explosion areas at the estimated times of the explosions. An analysis of the data revealed that the magnitudes of the strikes ranged from 16 kA to 112 kA [5].

Explosions can occur if lightning causes electric sparks with sufficient energy in a methane/air mixture with methane concentrations between 5-15% [4]. (The minimum energy requirement of only 0.3 mJ occurs with a methane concentration of 8.5%.) Pockets of explosive methane/air mixtures are not uncommon in abandoned and sealed areas of coal mines. Lightning-related sparking underground can result from transient voltage surges on metal structures, such as conveyors or rails, where small discontinuities occur within the structure. It is also believed that the dissipation of lightning in rock strata may cause sparks with sufficient energy to ignite a methane/air mixture [1].

Lightning can penetrate an underground mine by two mechanisms – propagation through the overlying strata and conduction through metallic structures extending from the surface to the mine [1]. With the first mechanism, a lightning strike at the surface propagates downward through the earth in a radial fashion. Analyses of tunneling accidents in the Swiss Alps show that lightning strikes are capable of penetrating significant depths of overburden with enough energy to detonate explosives [6]. The depth of penetration was shown to be proportional to soil resistivity. In other words, lightning will penetrate deeper in soils with higher resistivity. Uniformly elevating the soil's potential, with respect to remote earth, by itself may not necessarily create problems since potential differences are not present in localized areas. However, large conductive structures that are grounded at remote locations can distort local current distributions and result in potential gradients. Geological faults, although not discussed in this paper, can also significantly distort current distribution through the overburden.

The second lightning-penetration mechanism results from a direct strike to a metallic structure that extends from the surface to the mine, such as cables, conveyor structures, water pipes, and borehole casings. The attenuation of such a strike depends on the surge impedance of the structure and how effectively the structure is grounded.

This paper addresses both lightning propagation methods. A simplified model of an abandoned area of a coal mine is created. Rails from the underground transportation system are used as conductive structures that are grounded at remote locations, and a row of 6-ft roof bolts is positioned perpendicular to the rails. A double-exponential current surge is used to simulate a lightning strike and is injected into the earth at the surface. The CDEGS software first performs a Fast Fourier Transform (FFT) to convert the lightning strike from the time domain to the frequency domain. Current distributions, scalar potentials, and electromagnetic fields are then computed for selected frequencies at specified observation points. This information provides insight into the frequency response of the earth and associated metal conductors. Finally, an inverse FFT is then used to obtain time-domain ground potential rises (GPR) for specified conductor segments in the system. Computational methods for the CDEGS software can be found in references [7], [8], and [9].

II. MODEL DEVELOPMENT

A. Physical Model

The physical model is structured to create a situation where the GPR (ground potential rise) can be calculated at two nearby conductor segments to determine if a significant potential difference exists. A worst-case scenario would be if one conductor segment were part of a tire-mounted mining machine whose frame is tied to the safety ground bed on the surface, which could be a few miles from the equipment location. However, the explosions occurred in sealed areas, and cables and conductors are not permitted to extend beyond this area. Therefore, a more realistic situation was selected in which the two conductor segments reside in a rail and a roof bolt, with the roof bolt being located directly above the rail. Fig. 1 depicts the situation to be modeled and consists of a partially caved area of a coal mine. The plan view of Fig. 1 shows a 4000 ft by 4000 ft area to be modeled. The rail system spans the area in the x direction, while the roof bolts span the area in the y direction. A 500-ft length of the rail system on each end is located under caved material, while the remaining center portion of the track entry remains open. Thus the rails are essentially grounded at remote locations, with respect to the roof bolts. The roof-bolt entry remains open so that the roof bolts are located a few feet above the rails in the z direction, as shown in the side view of Fig. 1. The side view also shows the strike point where the voltage surge enters the earth, directly above the crossover point of the rails and the roof bolts.

The actual model was simplified to reduce the number of conductor segments, which in turn reduces the simulation time. (The maximum length of a conductor segment was set at 10 ft, which is less than one-sixth the wavelength of the highest frequency expected. Even with the simplified model, processing time can exceed 24 hr for each simulation when run on a Pentium™ III computer.) Figure 2 shows the simplified model for the situation defined in Fig. 1. A single, cylindrical rail, with the same cross-sectional area of a typical 60-lb/yd rail, is used instead of two separate rails. Since the portion of the CDEGS software used for this study does not permit modeling of void areas in the earth, such as mine openings, some approximations have to be used to model this situation. To accommodate this limitation, the 3000-ft center portion of the rail is modeled as a coated conductor, with a 1-ft thick coating. The coating is assigned the same resistivity and permitivity as air. The 500-ft end portions of the rail are left uncoated in intimate contact with the soil. Again, to reduce the number of conductor segments, only a single row of roof bolts is used. Steel conductors, 6-ft long with a 5/8-in. diameter, are used to model the roof bolts. The steel conductors for the rail and the roof bolts are assigned a relative resistivity of 17 and a relative permeability of 300. A copper rod, driven three feet into the earth, is located on the surface directly above the crossover point of the roof bolts and rail. This rod is used for injecting the lightning surge into the earth for *Scenario 1*. An observation surface is positioned horizontally, between the roof bolts and the rail. The intersecting points of the observation grid are used to calculate the scalar potentials in the soil.

Typical overburden consists of many layers of various types of strata, and the resistivity of each layer can vary dramatically. The composition of overburden is site specific, and discontinuities and geological faults can affect its electrical properties. However, to make the problem manageable, a uniform layer of soil, with a 400 Ω-m resistivity, is used to model the overburden.

A steel-cased borehole is used in *Scenario 2*. The borehole, not shown in Figs. 1 or 2, extends from the strike point on the surface to within a foot of a roof bolt. The borehole casing was modeled as a 6-in diameter pipe with an interior diameter of 5 in. Similar to the rails, the casing was assigned a relative resistivity 17 and a relative permeability of 300.

B. Lightning Surge

A magnitude of 84 kA was selected for the lightning strike. This value is 75% of the highest value obtained from the National Lightning Detection Network data. The lightning surge was modeled as a current source with the following double exponential function:

$$I(t) = I_m \left[e^{-\alpha t} - e^{-\beta t} \right] \qquad (1)$$

with

$I_m = 85.69$ kA,
$\alpha = 1.42 \times 10^4$, and
$\beta = 4.88 \times 10^6$.

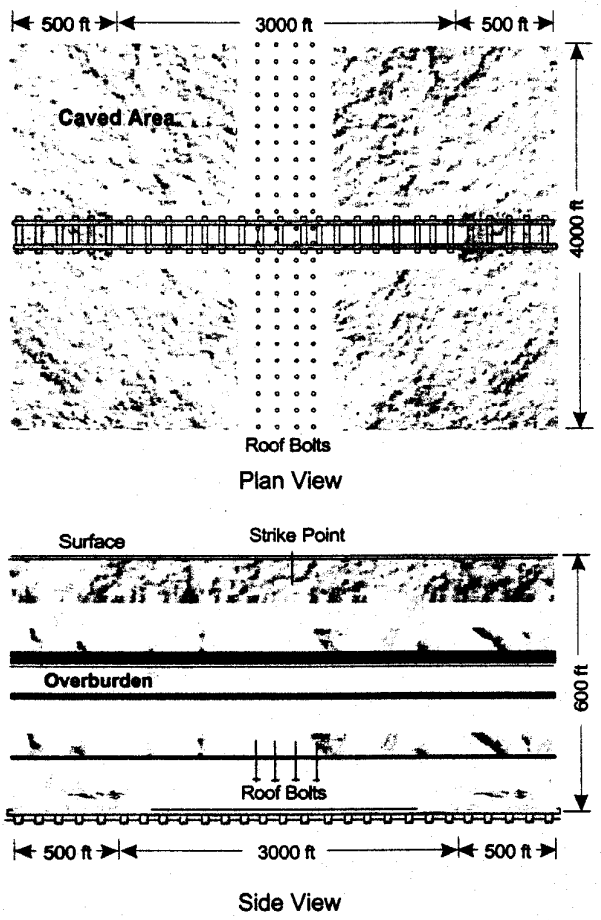

Fig. 1. Partially caved area of a coal mine to be modeled.

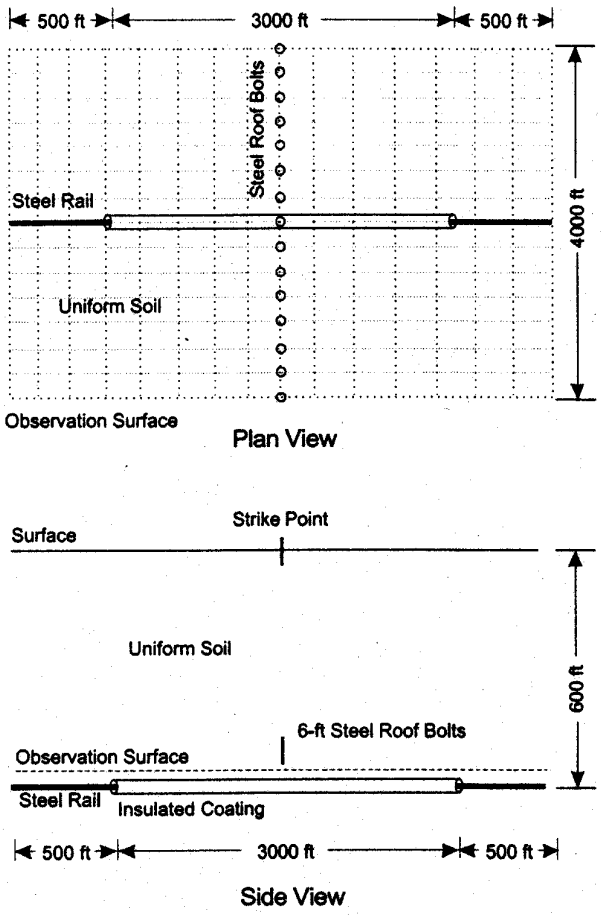

Fig. 2 Simulation model for Fig. 1.

These values result in a rise time of 1.2 μs to a peak current value of 84 kA. The surge decays to 50% of its peak value (42 kA) at 50 μs, as shown in Fig. 3a. Figure 3b shows that the waveform essentially decays to zero at 600 μs. This type of waveform is typically used for modeling lightning strikes [10].

III. Computer Simulations

The CDEGS software first uses a forward FFT to decompose the time-domain lightning surge of Fig. 3 into its frequency spectrum. It then selects a finite number of frequencies from this spectrum, based on the electromagnetic field response in the frequency domain. More frequencies with finer steps are selected in the regions where rapid changes occur. Electromagnetic fields are computed for defined observation points at each selected frequency to obtain the frequency spectrum of the fields. Finally, an inverse FFT is applied to the frequency spectrum of the computed electromagnetic fields, at the defined observation points, to yield the time-domain responses of the fields [9]. Simulations are performed for two scenarios. Figure 1 shows the physical model that is simulated in *Scenario 1*. *Scenario 2* is identical to *Scenario 1*, except that a steel-cased borehole is placed from the surface to within a foot of a roof bolt. The borehole is in intimate contact with the overburden for its entire length.

A. Scenario 1

Figure 2 depicts the model for *Scenario 1*. The frequency spectrum of the lightning surge in Fig. 3 ranges from dc to the mega-hertz range. Therefore, the model's unmodulated frequency response is first investigated. As an illustration, a per-unit current of $1.0 + j0.0$ *A* is injected into the strike point at the following frequencies: dc, 10 Hz, 100 Hz, and 1 kHz. Scalar potentials, based on the per-unit current, are calculated for each frequency at the intersecting points of the observation surface, illustrated in Fig. 2. The observation surface is a horizontal grid, located between the rail and the roof bolts, and consists of 81 profiles, with 81 points per profile. This arrangement results in a total of 6561 observation points, spanning the 4000 ft x 4000 ft area with a 50-ft spacing between adjacent points in the x and y directions. Figures 4, 5, 6, and 7 show the system's response to the per-unit current at the specified frequencies,

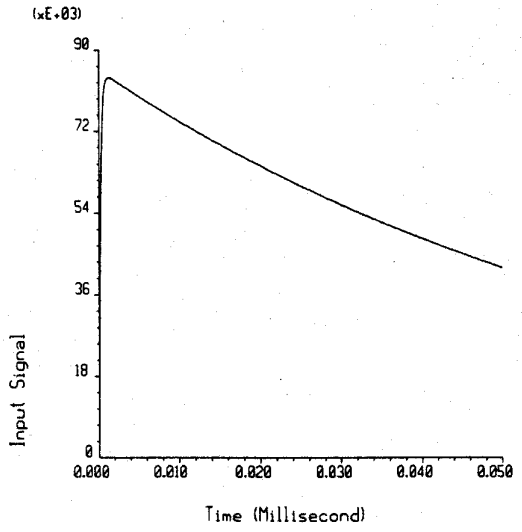

(a)

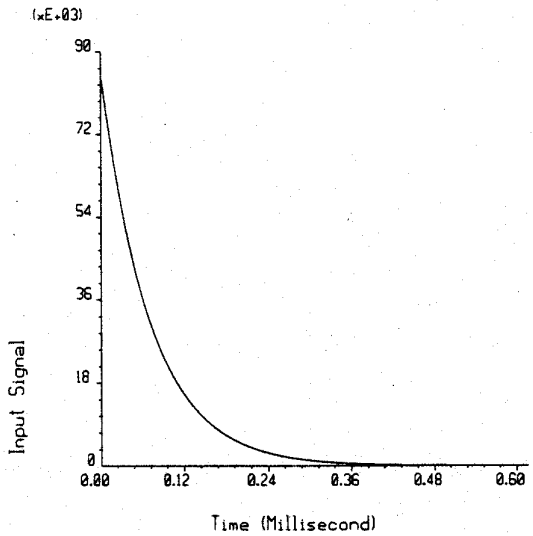

(b)

Fig. 3. Model of the lightning surge current.

respectively. Figures 4, 5, and 6 show that the three-dimensional perspectives for the scalar potentials at dc, 10 Hz, and 100 Hz are essentially the same, with peak values of approximately 0.35 V. Note the small distortion to the scalar potentials at dc and 10 Hz, due to the presence of the rail. This distortion essentially disappears at frequencies of 100 Hz and above. Attenuation of the scalar potentials becomes noticeable at 1 kHz, as shown in Fig. 7. The frequency spectrums (dc to 120 kHz) for the real and imaginary parts of the unmodulated scalar potentials are shown in Fig. 8.

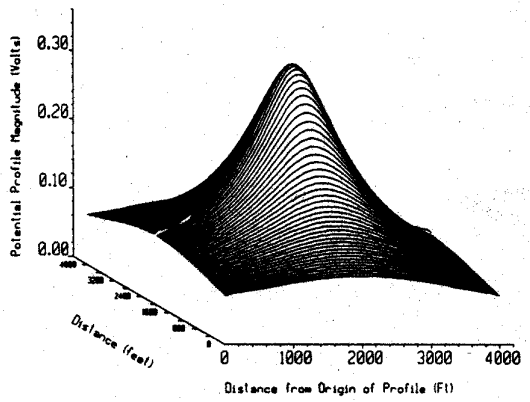

Fig. 4. Per-unit scalar potentials at dc for Scenario 1.

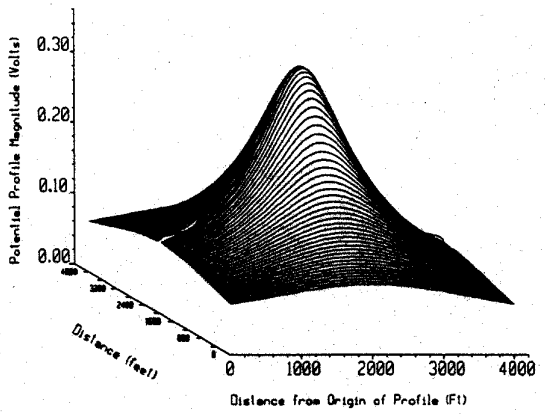

Fig. 5. Per-unit scalar potentials at 10 Hz for Scenario 1.

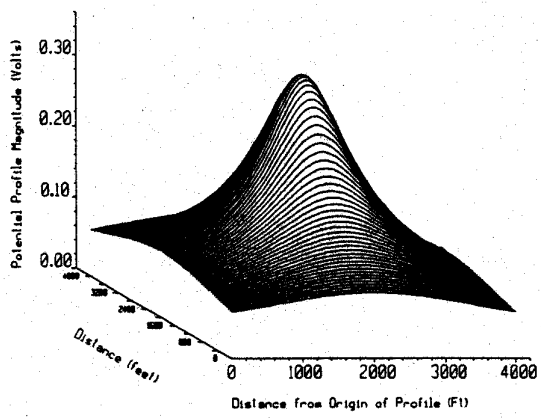

Fig. 6. Per-unit scalar potentials at 100 Hz for Scenario 1.

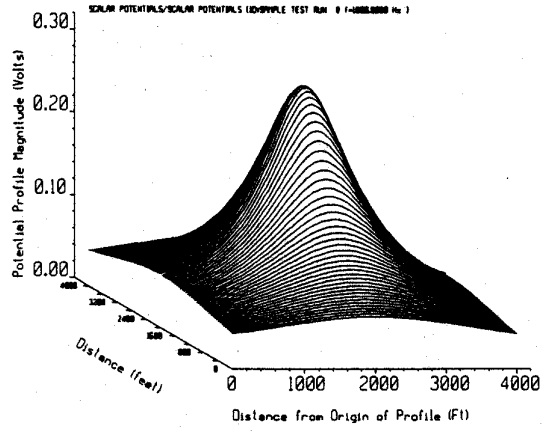

Fig. 7. Per-unit scalar potential at 1 kHz for Scenario 1.

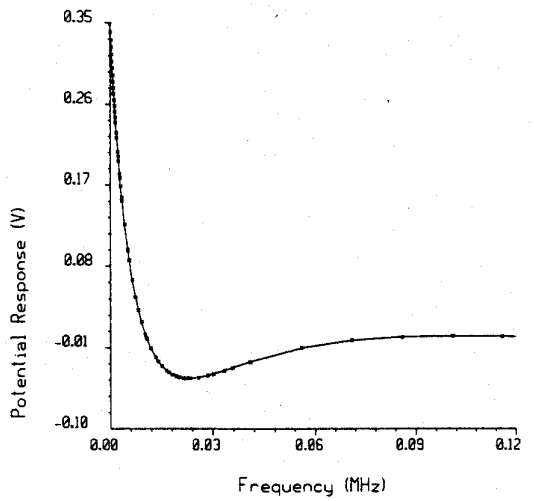

(a) Real part

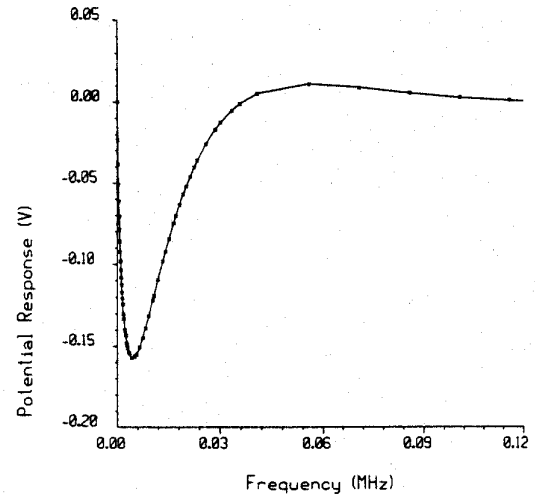

(b) Imaginary part

Fig. 8. Frequency spectrum of the unmodulated scalar potentials for Scenario 1.

Figure 8 shows that currents with frequencies above 100 kHz are essentially dissipated in the overburden prior to reaching the depth of the observation surface. Also frequencies below the 10-kHz range yield the greatest responses.

Figures 9, 10, and 11 show the per-unit GPRs for the conductor segments in the rail and the roof bolts at frequencies of dc, 10 Hz, and 100 Hz, respectively. A significant potential difference occurs between the roof bolts and the rail at the crossover point for dc and 10 Hz, as shown in Figs. 9 and 10. However, this potential difference vanishes at frequencies of 100 Hz and above, as shown in Fig. 11. Thus, the potential difference between the conductor segments is due solely to very-low frequency components.

An inverse FFT is used to compute the time-domain GPR in the roof-bolt and rail conductor segments at the crossover point, and the results are shown in Figs. 12 and 13, respectively.

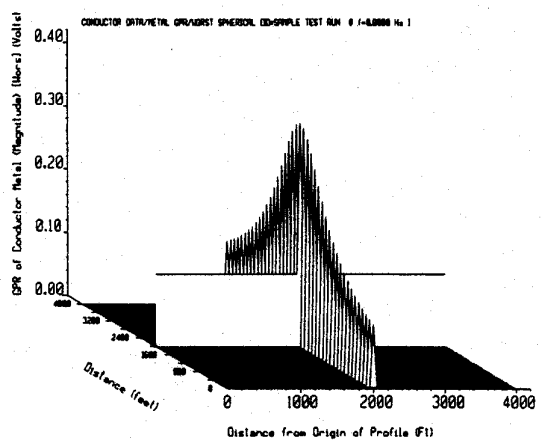

Fig. 9. GPR of rail and roof bolt segments at dc for Scenario 1.

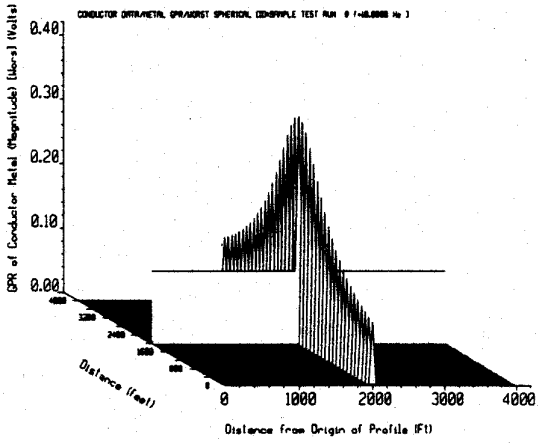

Fig. 10. GPR of rail and roof bolt segments at 10 Hz for Scenario 1.

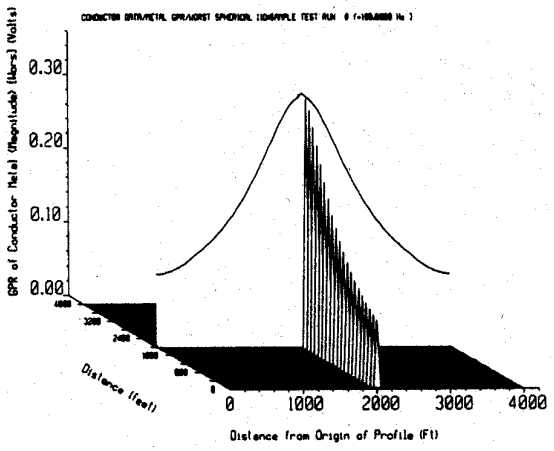

Fig. 11. GPR of rail and roof bolt segments at 100 Hz for Scenario 1.

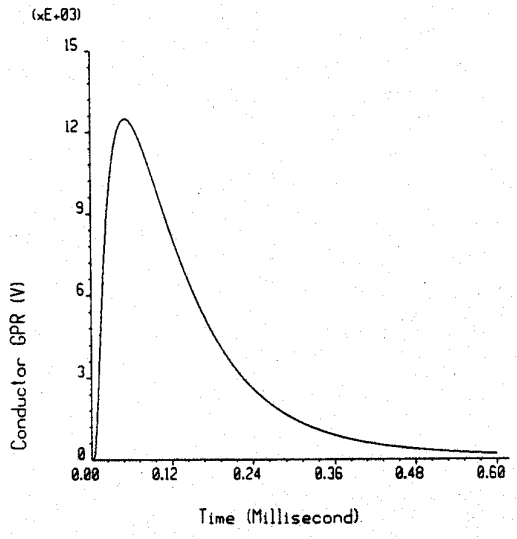

Fig. 12. Time-domain GPR of roof bolt at the roof-bolt/rail crossover point for Scenario 1.

The peak potential at the roof bolt is slightly greater than that of the rail, but both are near 12 kV. The waveform of Fig. 13 is subtracted from that of Fig. 12 in order to obtain the potential difference between the roof bolt and the rail, with the resulting waveform shown in Fig. 14. The potential difference has a peak value of 375 V. This voltage is certainly capable of generating an arc, but is relative small compared to the two GPRs. Given the assumptions and approximations made for defining this problem, as well as the limitations of the software, it is felt that this value does not provide conclusive evidence that the lightning strike is capable of initiating an explosion in *Scenario 1*.

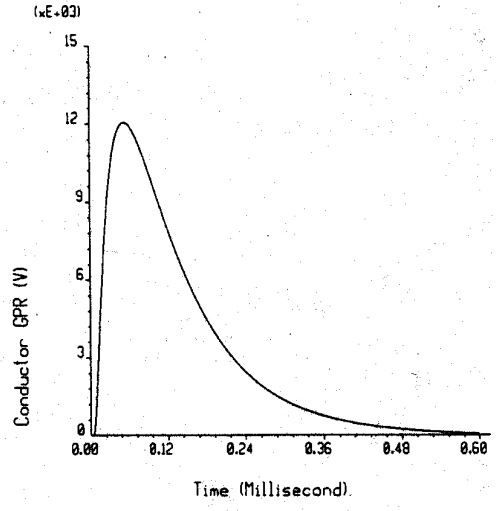

Fig. 13. Time-domain GPR of rail at the roof-bolt/rail crossover point for Scenario 1.

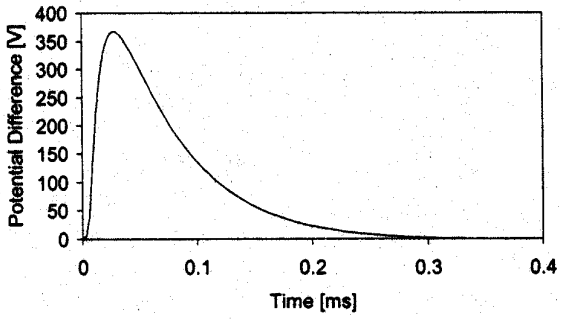

Fig. 14. Potential difference between roof bolt and rail for Scenario 1.

B. Scenario 2

Scenario 2 is essentially the same as *Scenario 1*, except that a steel-cased borehole, which extends from the surface to within one foot of a roof bolt, is included in the simulation model. As before, a per-unit current of *1.0 + j0.0 A* is injected into the strike point, and the borehole casing. The frequency spectrums (dc to 120 kHz) for the real and imaginary parts of the unmodulated scalar potentials are shown in Fig. 15. Similar to *Scenario 1*, currents with frequencies above 100 kHz are dissipated in the overburden prior to reaching the depth of the observation surface. For this scenario, frequencies below the 30-kHz range cause the greatest responses. As expected, the magnitudes of the unmodulated scalar potentials are significantly larger than those in *Scenario 1*. The time-domain GPRs in the roof-bolt

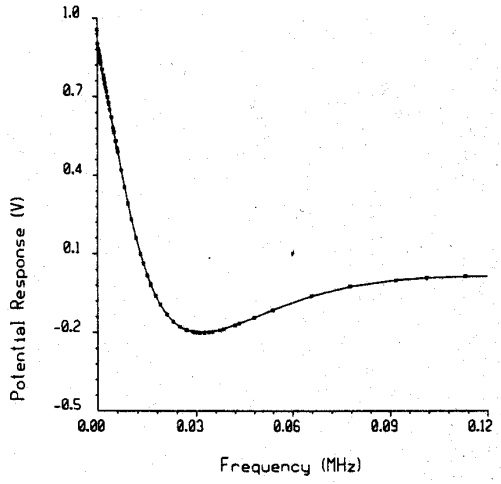

(a) Real part

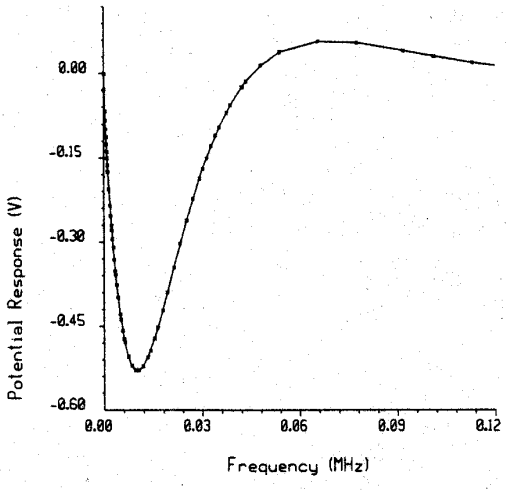

(b) Imaginary part

Fig. 15. Frequency spectrum of the unmodulated scalar potentials for Scenario 2.

and rail conductor segments at the crossover point are shown in Figs. 16 and 17, respectively. The peak potentials in the roof bolt and rail have dramatically increased to 57 kV and 40 kV, respectively. The potential difference between the two conductor segments has a peak value of 15.6 kV and is presented in Fig. 18. Even with the assumptions and approximations made for defining this problem, the magnitude of this potential difference provides convincing evidence that the lightning strike is capable of initiating an explosion in *Scenario 2,* depending on the arrangement of conductors and physical conditions within the mine area.

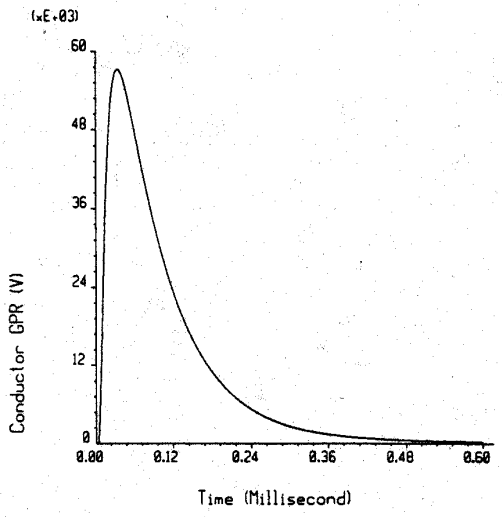

Fig. 16. Time-domain GPR of roof bolt at the roof-bolt/rail crossover point for Scenario 2.

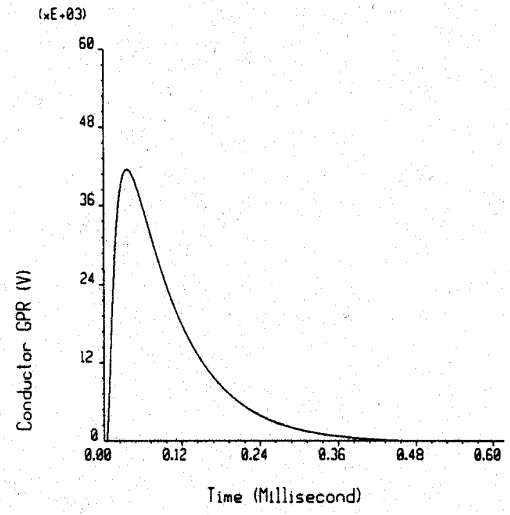

Fig. 17. Time-domain GPR of rail at the roof-bolt/rail crossover point for Scenario 2.

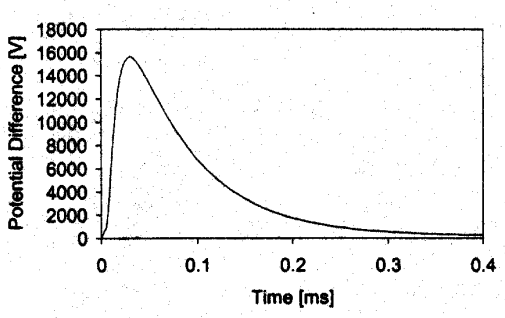

Fig. 18. Potential difference for Scenario 2.

IV. CONCLUSIONS

Two scenarios for a simplified model of an abandoned area of a coal mine were simulated. Rails from the underground transportation system were used as conductive structures that are grounded at remote locations, and a row of 6-ft roof bolts were positioned perpendicular to the rails. With *Scenario 1*, lightning was injected directly into the earth. A steel-cased borehole was added for *Scenario 2*. A double-exponential current surge, with a peak value of 84 kA, was used to simulate a lightning strike. CDEGS software from Safe Engineering Services & Technologies, Ltd was used for the simulations. CDEGS performed a Fast Fourier Transform (FFT) to convert the lightning strike from the time domain to the frequency domain. Current distributions, scalar potentials, and electromagnetic fields were computed for selected frequencies at specified observation points. An inverse FFT was used to obtain time-domain ground potential rises (GPRs) for specified conductor segments in the system.

The simulations showed that currents with frequencies below 10 kHz for *Scenario 1* and 30 kHz for *Scenario 2* cause the greatest contribution to the scalar potentials in the mine area. Peak values of 12 kV and 57 kV occurred between the roof bolt and remote earth for *Scenario 1* and *Scenario 2*, respectively.

For both scenarios, the potential differences between the roof-bolt and rail segments were solely due to very-low frequency currents, below 100 Hz. Values of 375 V for *Scenario 1* and 15.6 kV for *Scenario 2* were calculated. Given the assumptions and approximations made for defining this problem, as well as the limitations associated with any simulations, the authors feel that *Scenario 1* does not provide conclusive evidence that the lightning strike is capable of initiating an explosion and that further investigations need to be performed. However, *Scenario 2* presents very strong evidence that the presence of a steel-cased borehole dramatically enhances the possibility of lightning initiating an explosion in a mine at a 600-ft depth.

Future work will address the sensitivity of the model parameters, such as soil resistivity, depth of overburden, and diameter of the borehole casing. Simplified simulations will also be compared with a theoretical model to determine their level of agreement.

V. REFERENCES

[1] Geldenhuys, H.J., A.J. Eriksson, W.B. Jackson, and J.B. Raath, "Research into Lightning-Related Incidents in Shallow South African Coal Mines," *Proceedings of the 21st International Conference of Safety in Mines Research Institutes*, Sydney, Australia, October 1985.

[2] Geldenhuys, H.J., "The Measurement of Underground Lightning-Induced Surges in a Colliery," *Proceedings of the Symposium on Safety in Coal Mining, Pretoria, South Africa*, October 1987.

[3] Zeh, K.A., "Lightning and Safety in Shallow Coal Mines," *Proceedings of the 23rd International Conference of Safety in Mines Research Institutes*, Washington, D.C., September 1989.

[4] Golledge, P., "Sources and Facility of Ignition in Coal Mines," Australian IMM, Illawarra Branch Symposium, 1981.

[5] Checca, E.L. and D.R. Zuchelli, "Lightning Stirkes and Mine Explosions," *Proceedings of the 7th US Mine Ventilation Symposium.*

[6] Berger, K., *Protection of Underground Blasting Operations*, Chapter 20 – "Lightning," Vol. 2, edited by R.H. Golde, Academic Press, London, 1977.

[7] Selby, A. and F.P. Dawalibi, "Determination of the Current Distribution in Energized Conductors for the Computation of Electromagnetic Fields," *Proceedings of the IEEE/PES 1993 Summer Meeting*, Paper No. 93 SM 427-5 PWRD.

[8] Dawalibi F.P. and A. Selby, "Electromagnetic Fields of Energized Conductors," *Proceedings of the IEEE/PES 1992 Summer Meeting*, Paper No. 92 SM 456-4 PWRD.

[9] Dawalibi, F.P., W. Ruan, and S. Fortin, "Lightning Transient Response of Communications Towers and Associated Grounding Networks," *Proceedings of the International Conference on Electromagnetic Compatibility*, 1995.

[10] Zipse, D.W., "Lightning Protection Systems: Advantages and Disadvantages," IEEE Transactions on Industry Applications, Vol. 30, No. 5, 1994, pp. 1351-1361.